

EVALUATING TIFFS (TOOLBOX FOR LIDAR DATA FILTERING AND FOREST STUDIES) IN DERIVING FOREST MEASUREMENTS FROM LIDAR DATA

JOHN CHAPMAN¹, I-KUAI HUNG², JEFF TIPPEN³

¹ Graduate Assistant, ² Associate Professor, Stephen F. Austin State University, Nacogdoches, TX 75962 USA

³ Senior Project Engineer, Surdex Corporation

ABSTRACT. Recent advances in LiDAR (Light Detection and Ranging) technology have allowed for the remote sensing of important forest characteristics to be more reliable and commercially available. Studies have shown that this technology can adequately estimate forest characteristics such as individual tree locations, tree heights, and crown diameters. These values are then used to estimate biophysical properties of forests, such as basal area and timber volume. This study assessed the capability of a commercially available program, Tiffs (Toolbox for Lidar Data Filtering and Forest Studies), to accurately estimate forest characteristics, as compared to data collected at the plot level using traditional timber sampling methods. We found a high, positive correlation coefficient (r) of 0.8223 for tree heights, between the LiDAR-derived measurements and the field measurements, which is somewhat promising. However, we found low correlations in tree count per plot ($r = 0.1777$) and tree crown radius ($r = 0.1517$), between the LiDAR-derived measurements and the field measurements, results which are far from satisfactory.

Keywords: LiDAR, remote sensing, forestry

1 INTRODUCTION

Remote sensing is an alternative method for obtaining spatial information, as compared to field-based measurements, which can be highly accurate but are time intensive and costly (Hyde *et al.* 2006). Aerial photography and satellite imagery have been implemented as remote sensing techniques for decades; however, they may require time-consuming and labor-intensive photogrammetric processes (Hyde *et al.* 2006). Further, these processes produce only two-dimensional images, without the resolution and accuracy sufficient for obtaining three-dimensional information for vegetation (Omasa *et al.* 2007, Lefsky *et al.* 2002). Alternatively, LiDAR systems directly measure not only x and y coordinates, but z coordinates as well, increasing the accuracy of measurements and extending spatial analysis into the third dimension (Lefsky *et al.* 2002).

LiDAR (Light Detection and Ranging) is an innovative remote sensing tool that essentially measures distance with a laser. Distance is determined by measuring the travel time between an emitted and received pulse of light (Wehr and Lohr 1999). The travel time is the amount of time that elapses between the emission of a

light pulse, the reflectance of that pulse off of an object, and its recovery by the sensor (Wehr and Lohr 1999; Lim *et al.* 2003). These near-infrared laser pulses can be emitted at a high rate, exceeding 100,000 per second (Reutebuch *et al.* 2005, Evans *et al.* 2006). The pulse rate for the LiDAR system used in this study was 150 kHz. This technology is mounted to an aircraft in combination with an oscillating deflecting mirror to divert the beam to produce a wide-scan range and a Position and Orientation System (POS) to determine the locations of reflective surfaces (Wehr and Lohr 1999). The POS consists of a differential Global Positioning System (dGPS) that extrapolates the position of the sensor, and an Inertial Measurement Unit (IMU) to account for roll, pitch, and yaw in the aircraft (Wehr and Lohr 1999, Lim *et al.* 2003, Simard *et al.* 2003, Evans *et al.* 2006). The result is a set of points that give the horizontal and vertical position of each recorded return in Earth-referenced coordinates (Evans *et al.* 2006). This is also referred to as a point cloud. Wehr and Lohr (1999) provided a more in-depth exploration into how LiDAR systems work.

Several different systems are currently available to obtain LiDAR data, and new methods for processing the data, particularly software, are being implemented ev-

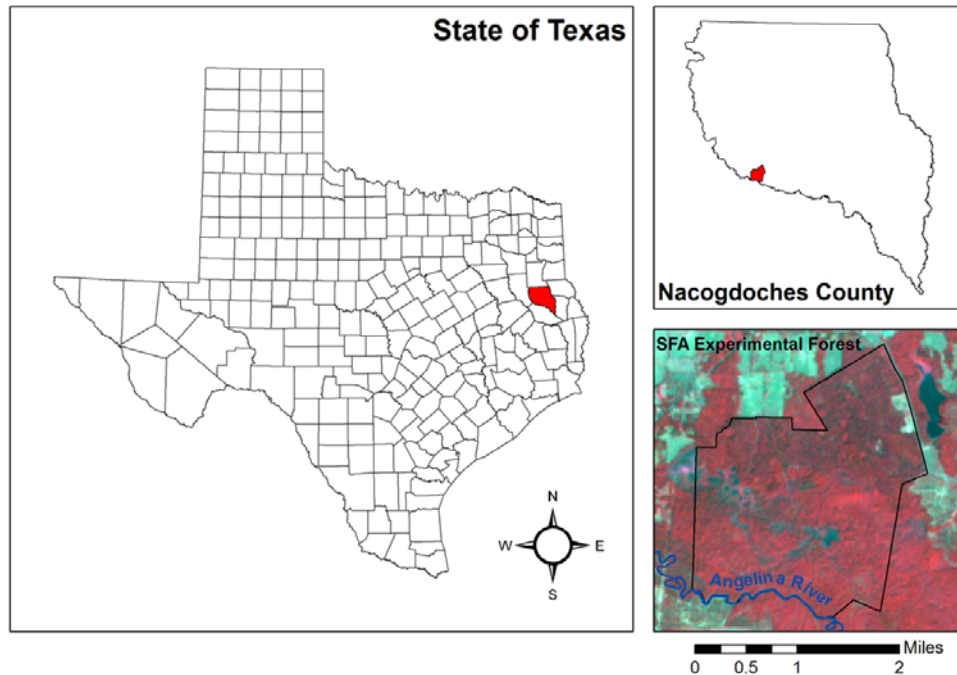


Figure 1: Location of the SFA Experimental Forest with color-infrared imagery.

ery day. With so many combinations of data acquisition and analysis, results of obtaining forest characteristics tend to vary. In the past, LiDAR was used mainly for terrain analysis and any returns of above-ground objects or trees were considered unwanted noise. Reutebuch *et al.* (2005) called for specifications and standards for LiDAR missions to allow for optimal remote sensing for not just terrain, but vegetation as well. As these standards are being implemented, studies need to be designed to evaluate the effects they have on accuracy.

The recent advances in LiDAR applications have allowed for the remote sensing of important forest characteristics to be increasingly accurate, affordable, and commercially available. Studies have shown this technology to be feasible in obtaining enough information to adequately estimate biophysical properties of forests, including stand volume and basal area (Means *et al.* 2000). Traditionally, these properties are estimated from field measurements, which are costly and time intensive to obtain, or 2-dimensional image processing, which allows one to estimate area but not volume. With LiDAR, these types of forest measurements can be captured remotely from a 3-dimensional perspective.

The purpose of this study is to provide some insight into the current capability of a commercially available software program, Toolbox for LiDAR data Filtering and Forests Studies (Tiffs). Tiffs is a product of Globalidar and it uses small-footprint LiDAR to estimate forest characteristics. The objective is to evaluate the cor-

relation between LiDAR measurements and field measurements. Thus the evaluation was performed using an accuracy assessment that compared the LiDAR-derived measurements from Tiffs against field samples obtained with conventional methods.

2 METHODS

2.1 Study Area and LiDAR Data Acquisition

The study area is the Stephen F. Austin (SFA) Experimental Forest in Nacogdoches County, Texas, part of the Angelina National Forest. It was established by the U.S. Congress on December 14, 1944 and transferred to the U.S Forest Service for the purpose of cooperating with forestry-related research conducted by Stephen F. Austin State University (Russell 2002). The area consists of roughly 1,036 ha (2,560 acres) along the Angelina River, composed of southern bottomland hardwoods, southern pine, and mixed pine-hardwood forests. The elevation ranges from 53 to 80 m (173 to 263 ft) above mean sea level (Figure 1).

In cooperation with Stephen F. Austin State University, the Surdex Corporation conducted a LiDAR flight mission over the SFA Experimental Forest. The data were obtained on August 15th, 2007, using a Leica ALS50-II LiDAR system that captured discrete, multiple-return data with an average point density of 5.67 points per m². This dataset was delivered in LAS format. Each LAS file covers a square area of 250 by

250 m.

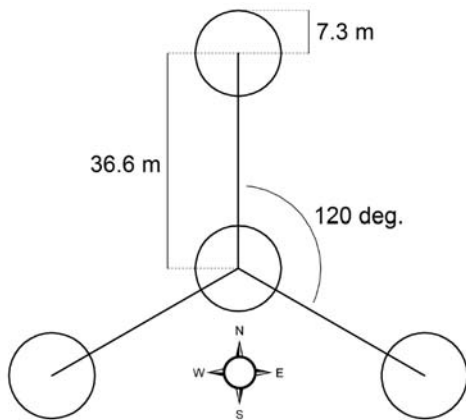


Figure 2: FIA (Forest Inventory and Analysis) plot layout.

2.2 Hardware and Field Measurement For sampling purposes, the entire SFA Experimental Forest was divided into 205 tiles, 250 by 250 m each, corresponding to the grid system of the LiDAR dataset. Each tile was classified as either pine, hardwood, or mixed forest as the result of a majority process run against a digital land cover map for a four-county study in east Texas. The land cover map used for forest cover type classification of the tiles had an overall accuracy of 72.78%, and was derived from 30 m resolution Landsat ETM+ imagery (Unger *et al.* 2008). Thirty of these tiles were randomly selected, and stratified between the different cover types, with the primary focus on pine. Eleven tiles were selected from hardwood forests, fifteen from pine forests, and four from mixed forests. At the center of each tile, a plot was installed based on the sampling method outlined by the USDA Forest Inventory and Analysis (FIA) National Program. A FIA plot consists of four circular subplots; a center subplot and three subplots 36.6 m away from the center, 120° apart (Figure 2). Each circular subplot has a radius of 7.3 m (Burkman 2005).

For field data collection, a map of the study area was created with ArcGIS, and contained reference data such as roads, streams, and imagery (Figure 3). The map also contained the LiDAR tiles and a layer that contained the measured tree data. This map, along with its data, was transferred to a Trimble Recon handheld unit where data was entered in the field with the assistance of ArcPad software. With a Trimble Pro-XR GPS receiver, all trees with a DBH greater than 15.24 cm (6 inches) were mapped using the UTM coordinate system, NAD 1983. The height of each tree was measured using a Trupulse 200B rangefinder from Laser Technology Inc. Tree crown radii in the four cardinal directions (N, S, E, W) were

also measured with the rangefinder by positioning the unit underneath the edge of the crown and measuring the physical distance back to the tree trunk. Diameter at breast height (DBH) was measured using a diameter tape. For each tree measured, its status (alive or dead), species (generalized between pine and hardwood), and the date of data collection were recorded. To assist in the use of the rangefinder, and to provide greater accuracy, a retro-reflector surveyor's prism mounted on a staff was used. A staff-compass was used to determine the locations of the sub-plots within each plot. The data collection was performed between May 2008 and May 2009. A total of 603 trees were measured.

2.3 Data Processing Tiffs (Toolbox for LiDAR Data Filtering and Forest Studies) is a commercially available software program that uses an automated extraction process to generate digital surface models (DSM), digital elevation models (DEM), and canopy or object height models (CHM/OHM) based on LiDAR data input (Chen 2007). The DSM is a raster layer that represents the elevation of the canopy. The DEM provides the elevation surface of the LiDAR returns that the software has deemed ground-returns, depicting the bare-earth terrain. The software then subtracts the DEM from the DSM to generate the CHM, which represents the height of the canopy above the bare ground. Tiffs then uses the CHM to isolate individual trees using a marker-controlled watershed segmentation method, and provides their location, height, and crown diameter (Chen *et al.* 2006, Chen 2007). This process was performed on each of the 30 randomly selected data tiles, and all LiDAR return values were used.

Other than generating DSM, DEM, and CHM in raster format, Tiffs also created a text file containing height, crown diameter, and the x , y , and z coordinates of each individual tree identified in each data tile. The text files were converted to ESRI point shapefiles containing all trees and their associated attributes. The LiDAR-derived trees that fell within the boundary of the sample plots were selected and extracted for comparison against the field-measured tree data. A total of 1,541 trees that were derived from the LiDAR were within the sample plots.

2.4 Forest Statistics Three parameters (number of trees per plot, average tree height per plot, and average crown radius per plot) were used to compare the LiDAR-derived and the field-measured data. For each parameter, root mean square error (RMSE) and correlation coefficients (r) were calculated based on the assumption that the field-measured data are accurate. Each RMSE was converted to the percentage of the field-measured mean value, representing the magnitude of er-

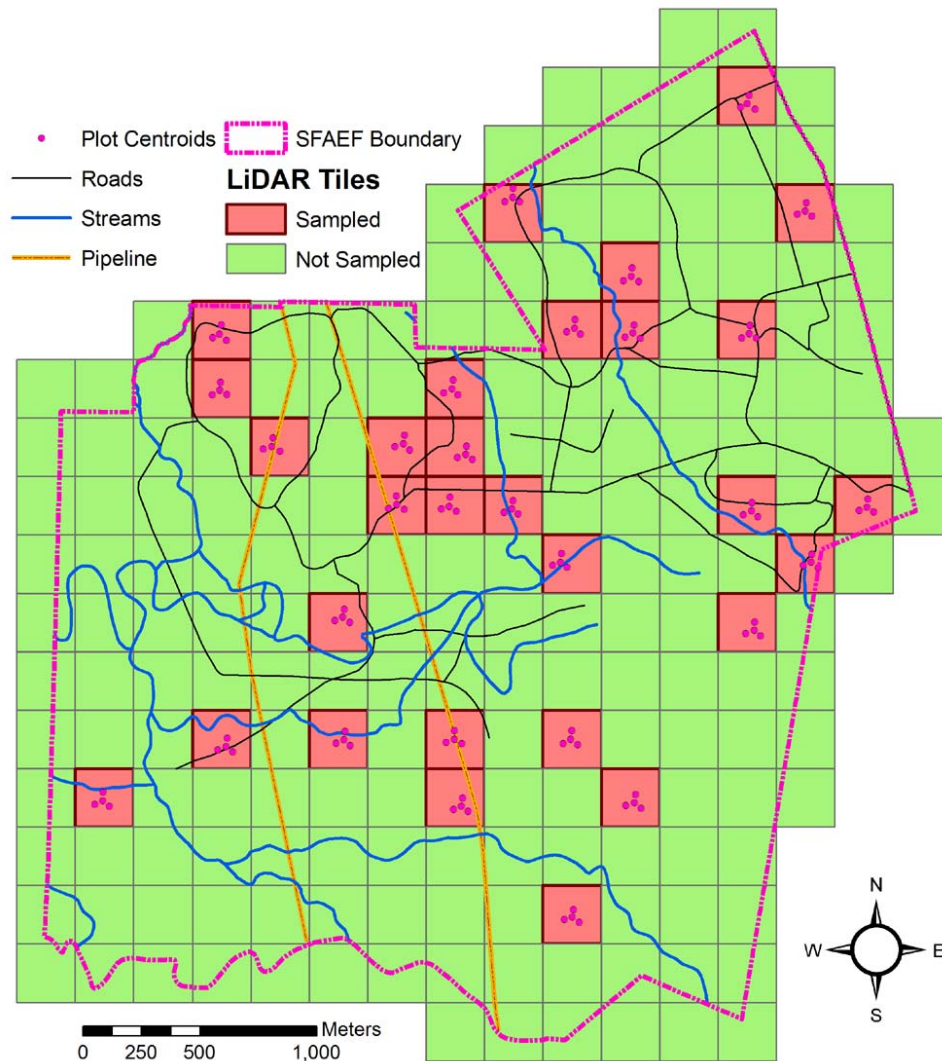


Figure 3: Map of the SFA Experimental Forest used for field data collection.

ror (Figure 4). The correlation coefficient, or r -statistic, was calculated between the LiDAR-derived and the field-measured measurements. In general, the higher the correlation coefficient, more accurate the LiDAR data estimation process. Both the RMSE and the correlation coefficient (r) were calculated at the plot and sub-plot level using both unfiltered data and filtered data. The filtered data were obtained by removing field-measured trees that were classified as dead and having no crown to measure. Since trees with a DBH of less than 15.24 cm (6 inches) were not measured in the field plots, LiDAR-derived trees with height less than 7 m were removed from the analysis, with the assumption that trees less than 7 m tall would have a DBH of less than 15.24 cm (6 inches). This threshold was determined based on the correlation between tree height and DBH from the field-measured data.

3 RESULTS AND DISCUSSION

The correlation between LiDAR-derived and field-measured data was generally highest when using the unfiltered data and when viewed at the plot level (Table 1). When all trees were considered, r for tree count was 0.1777. However, when looking at specific forest types, the r -values were 0.2569, 0.0855, 0.7156 for pine, hardwood, and mixed forests, respectively (Table 1, Count). It is obvious that the LiDAR-derived data suggested that there were more trees present than what were measured in the field, with the average number of trees per plot always being greater than that of the field measurements. This resulted in significant errors (all greater than 100%) in tree counts. Since the Tiffs analysis process is based on the peaks in the canopy height model, when locating trees from LiDAR data, any spike in the canopy could

Table 1: Comparison of forest measurements between LiDAR-derived and field-measured data.

		Count						
		n	Mean _{Field}	Mean _{LiDAR}	RMSE	% Error	r	
Plot Level	Non-Filtered:	All	30	20.1	50.7	32.0687	159.55	0.1777
		Pine	15	17.8	52.9	30.2798	170.11	0.2569
		Hardwood	11	20.8	49.5	36.1210	173.66	0.0855
		Mixed	4	23.8	49.0	26.2059	110.11	0.7156
	Filtered:	All	29	19.1	49.9	31.9137	167.09	0.3081
		Pine	15	20.1	50.0	30.8275	153.37	0.2838
		Hardwood	10	16.5	50.2	35.0386	212.36	0.4668
		Mixed	4	22.0	48.5	27.4044	124.57	0.6962
Sub-Plot Level	Non-Filtered:	All	120	5.1	12.8	8.8704	173.93	0.0591
		Pine	60	5.4	12.7	8.6178	159.59	0.1412
		Hardwood	44	4.5	13.2	9.5679	212.62	0.0684
		Mixed	16	6.1	12.3	7.7379	126.85	-0.1604
	Filtered:	All	116	4.8	12.5	8.9139	185.71	0.1240
		Pine	60	5.0	12.5	8.6766	173.53	0.1734
		Hardwood	40	4.1	12.6	9.4657	230.87	0.2724
		Mixed	16	5.5	12.1	8.3516	151.85	-0.3458
		Height (m)						
Plot Level	Non-Filtered:	All	30	20.5	24.9	5.4493	26.58	0.8223
		Pine	15	17.3	21.9	5.3513	30.93	0.7363
		Hardwood	11	22.7	27.0	5.3256	23.46	0.8601
		Mixed	4	21.2	25.6	6.1098	28.82	0.9429
	Filtered:	All	29	21.4	26.1	5.6517	26.41	0.7517
		Pine	15	23.0	27.4	5.3842	23.41	0.7584
		Hardwood	10	18.8	24.2	6.0313	32.08	0.6031
		Mixed	4	21.9	25.9	5.6502	25.80	0.9754
Sub-Plot Level	Non-Filtered:	All	120	19.7	24.6	7.7536	39.36	0.6458
		Pine	60	22.6	26.6	6.6482	29.42	0.6077
		Hardwood	44	16.2	21.5	7.2251	44.60	0.4954
		Mixed	16	18.8	25.9	10.9953	58.49	0.3964
	Filtered:	All	116	20.5	25.7	7.9771	38.91	0.5316
		Pine	60	22.5	27.1	7.6040	33.80	0.5121
		Hardwood	40	18.1	23.6	7.1417	39.46	0.3116
		Mixed	16	19.2	26.0	10.8168	56.34	0.3881
		Crown Radius (m)						
Plot Level	Non-Filtered:	All	30	3.2	1.5	1.8818	58.81	0.1517
		Pine	15	3.0	1.5	1.8272	60.91	0.1065
		Hardwood	11	3.3	1.6	1.8976	57.50	0.0798
		Mixed	4	3.5	1.6	2.0335	58.10	0.1464
	Filtered:	All	29	3.5	1.6	2.0780	59.37	-0.0985
		Pine	15	3.4	1.6	1.9149	56.32	0.0693
		Hardwood	10	3.6	1.5	2.1927	60.91	-0.5537
		Mixed	4	3.8	1.6	2.3527	61.91	0.2561
Sub-Plot Level	Non-Filtered:	All	120	3.2	1.6	2.0574	64.29	0.0842
		Pine	60	3.4	1.6	2.0707	60.90	0.0462
		Hardwood	44	3.0	1.5	2.0411	68.04	0.0036
		Mixed	16	3.2	1.6	2.0517	64.12	0.2055
	Filtered:	All	116	3.5	1.6	2.2241	63.55	-0.1062
		Pine	60	3.5	1.7	2.2162	63.32	-0.1733
		Hardwood	40	3.5	1.6	2.1880	62.51	-0.2139
		Mixed	16	3.5	1.7	2.3403	66.87	0.2827

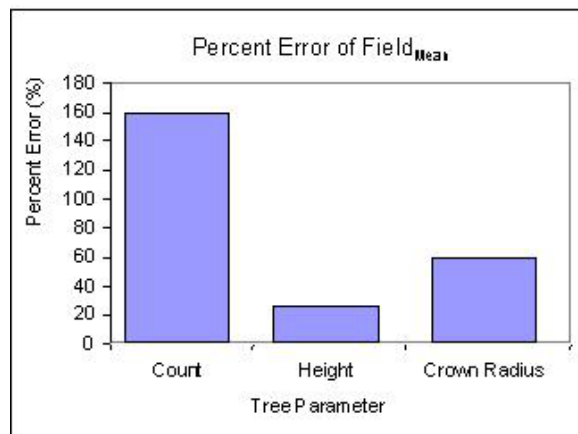


Figure 4: Comparison of percent error among tree parameters based on the field mean.

be misidentified as an individual tree. The low correlation between the LiDAR-derived and the field-measured data for identifying trees also poses a problem when estimating the timber volume of a stand. Unfortunately, the Tiffs program offered limited functionality for calibration.

For tree heights, the correlation using all trees at the plot level was relatively high ($r = 0.8223$) (Table 1, Height). When focusing on specific forest types, the r -values were 0.7363, 0.8601, 0.9429 for pine, hardwood, and mixed forests, respectively. For comparison purposes, Means *et al.* (2000), in their study of Douglas-fir in the western Cascades of Oregon, were able to achieve an r -value of 0.96 ($R^2 = 0.93$) by using the average of the maximum heights of each 10 m grid cell when comparing LiDAR-derived tree heights to field-measured heights. Kwak *et al.* (2007), applied additional transformations to the watershed transformation as the basis for individual tree delineation, and obtained an r -value of 0.88 ($R^2 = .77$) for Korean pine trees in Central South Korea. Holmgren *et al.* (2003) created an interpolated surface of the LiDAR data to obtain vertical distance from the estimated ground elevation, and then used local maxima to obtain mean tree heights. In their study, an r -value of 0.95 ($R^2 = 0.90$) was achieved.

For our study, the correlation in tree height is fairly consistent with the findings from other studies mentioned above. However, the accuracy is still problematic when examining the RMSE of 5.4493 m (26.58%) when all trees were considered at the plot level (Table 1, Height). When comparing average tree height per plot, LiDAR-derived tree heights was greater than field-measured heights at all levels. This can be explained in that LiDAR detects tree heights based on the highest point of the canopy height model, whereas the tallest

point of a tree is usually difficult to see when measuring it in the field. Another possible cause is that LiDAR identified much larger number of trees than what was found in the field, which may bias the analysis towards higher values of the canopy. Traditionally, foresters measure merchantable height in timber cruise. If LiDAR is to complement field measurements by identifying individual trees, the tree height measurement needs to be calibrated carefully.

As for tree crown radius, the correlation coefficient for all trees at plot level was 0.1517, which is less than satisfactory (Table 1, Crown Radius). When examining specific forest types, the r -values were 0.1065, 0.0798, and 0.1464 for pine, hardwood, and mixed forests, respectively. When comparing the mean crown radius per plot, the LiDAR-derived measurements were always less than the field measurements. This problem is related to the fact that LiDAR identified more trees than what were found in the field. It is clear that LiDAR picked up more trees with limited overlapping crowns, while in reality there were actually fewer trees with larger crowns, which were often overlapping (Figure 5). This could be due to over-segmentation on the canopy height model when detecting individual trees (Kwak *et al.* 2007).

We also noticed that the r -value for the mixed forest type is greater than those of pine and hardwood for both tree count ($r = 0.7156$) and tree height ($r = 0.9429$) at the plot level (Tables 1, Count and Height). As tree detection is based on a continuous canopy height surface, the less homogeneous surface of the mixed forest allows for more accurate delineation of individual trees than those in pine and hardwood forests, which are generally more uniform in canopy structure.

4 CONCLUSIONS

While Tiffs estimation of tree height is promising, with a correlation coefficient of 0.8223, tree count and crown radius estimates appeared to be much less accurate. However, there was some consistency in the errors. Tiffs tends to overestimate the number of trees and underestimate the crown radius. Tiffs is an easy-to-use and affordable tool capable of analyzing LiDAR data, generating a DEM and a CHM, and also delineating individual trees with their attributes. All of these outputs are useful in describing the structure of a forest stand. However, the software lacks the ability of allowing the user to calibrate the process in order to increase accuracy.

Even though studies have shown promising results that LiDAR can be used for delineating individual trees and estimating forest properties with satisfactory accuracy, the performance of an algorithm might vary from one forest type to another, or from one region to an-

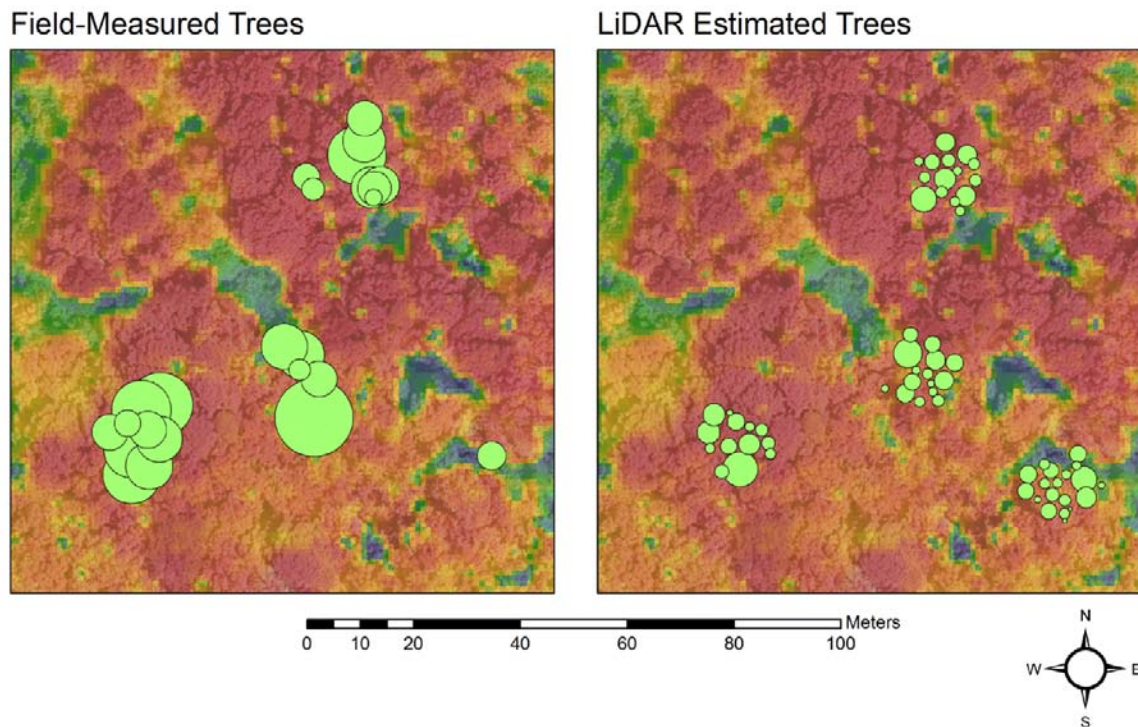


Figure 5: Crown radius comparison of field-measured trees and LiDAR-estimated trees.

other. As a commercially available LiDAR data processing program, it should be made clear what types of landscapes will work best with the software. In the meantime, allowing for the calibration of estimates in conjunction with field-measured training data would increase the accuracy. If a forest manager is to choose a LiDAR data processing software program for operational purposes, the ability to fine-tune the results is a criteria that should be considered in addition to the cost of the software.

ACKNOWLEDGEMENTS

The authors would like to thank the U.S. Forest Service for granting access to the SFA Experimental Forest. We appreciate the four anonymous reviewers for their invaluable comments and suggestions. This project was partially funded by the U.S. National Park Service and by the McIntire-Stennis grant.

REFERENCES

- Burkman, B. 2005. Forest inventory and analysis sampling and plot design. FIA Fact Sheet Series. Available at: <http://fia.fs.fed.us/library/fact-sheets/data-collections/Sampling%20and%20Plot%20Design.pdf>. Accessed on September 6, 2009.
- Chen, Q. 2007. Airborne lidar data processing and information extraction. *Photogrammetric Engineering & Remote Sensing*. 73(2):109-112.
- Chen, Q., D. Baldocchi, P. Gong, and M. Kelly. 2006. Isolating individual trees in a savanna woodland using small footprint lidar data. *Photogrammetric Engineering & Remote Sensing*. 72(8): 923-932.
- Evans, D. L., S. D. Roberts, and R. C. Parker. 2006. Lidar – a new tool for forest measurements? *The Forestry Chronicle*. 82(2):211-218.
- Holmgren, J., M. Nilsson, and H. Olsson. 2003. Estimation of tree height and stem volume on plots using airborne laser scanning. *Forest Science*. 49(3):419-428.
- Hyde, P., R. Dubayah, W. Walker, J. B. Blair, M. Hofton, and C. Hunsaker. 2006. Mapping forest structure for wildlife habitat analysis using multi-sensor (LiDAR, SAR/InSAR, ETM+, Quickbird) synergy. *Remote Sensing of Environment*. 102(1-2):63-73.
- Kwak, D., W. Lee, J. Lee, G. S. Biging, and P. Gong. 2007. Detection of individual trees and estimation of tree height using lidar data. *Journal of Forest Research*. 12(16): 425-434.

- Lefsky, M. A., W. B. Cohen, G. G. Parker, D. J. Harding. 2002. Lidar remote sensing for ecosystem studies. *BioScience*. 52(1):19-30.
- Lim, K., P. Treitz, W. Cohen, and M. Berterretche. 2003. Lidar remote sensing of forest structure. *Progress in Physical Geography*. 27(1):88-106.
- Means, J. E., S. A. Acker, B. J. Fitt, M. Renslow, L. Emerson, and C. J. Hendrix. 2000. Predicting forest stand characteristics with airborne scanning lidar. *Photogrammetric Engineering & Remote Sensing*. 66(11):1367-1371.
- Omasa, K., F. Hosoi, and A. Konishi. 2007. 3D lidar imaging for detecting and understanding plant responses and canopy structure. *Journal of Experimental Botany*. 58(4):881-898.
- Reutebuch, S. E., H. E. Anderson, and R. J. McGaughey. 2005. Light detection and ranging (lidar): an emerging tool for multiple resource inventory. *Journal of Forestry*. 103(6):286-292.
- Russell, C. C. 2002. An early history of the Stephen F. Austin Experimental Forest: utilizing interactive multimedia and oral histories. MS thesis, Stephen F. Austin State University, Nacogdoches, Texas.
- Simard, R., P. Belanger, M. R. Mohamed, and M. A. Othman. 2003. Airborne lidar surveys – an economic technology for terrain data acquisition. In: *Proceedings of the Map Asia Conference 2003*; 2003 Oct 13-15; Putra World Trade Centre, Kuala Lumpur, Malaysia. GISDevelopment.net.
- Unger, D., J. Kroll, I-K. Hung, J. Williams, D. Coble, and J. Grogan. 2008. A standardized, cost-effective, and repeatable remote sensing methodology to quantify forested resources in Texas. *Southern Journal of Applied Forestry*. 32(1):12-20.
- Wehr, A., and U. Lohr. 1999. Airborne laser scanning – an introduction and overview. *ISPRS Journal of Photogrammetry and Remote Sensing*. 54(2-3):68-82.